

**Supplementary Information**

Quantum rotational dynamics of *l-C<sub>4</sub>* (<sup>3</sup>Σ<sub>g</sub>) by H<sub>2</sub> at low temperatures  
employing machine learning augmented potential energy surface

*Pooja Chahal, Apoorv Kushwaha and T.J. Philip Kumar*

*Quantum Dynamics Lab, Department of Chemistry*

*Indian Institute of Technology Ropar, Rupnagar 140001, India*

## Table of Contents

<i>Table S1: Data of rate coefficients of excitation transitions for the comparison of para H<sub>2</sub> and ortho H<sub>2</sub> as a function of temperature.....</i>	<b>S3</b>
<i>Table S2: Data of rate coefficients of de-excitation transitions for the comparison of para H<sub>2</sub> and He as a function of temperature.....</i>	<b>S5</b>
<i>Table S3: Python program for generating PES.....</i>	<b>S7</b>
<i>Table S4: Ab initio energies (C<sub>4</sub>-H<sub>2</sub>) at various geometries compared to recreated PES (from radial terms). .....</i>	<b>S8</b>
<i>Table S5: Computed properties of C<sub>4</sub> compared to previous literature.....</i>	<b>S8</b>
<i>Figure S1: Cross-sections for the rotational excitation transitions (1-N) of collision of C<sub>4</sub> with ortho H<sub>2</sub> till energy range of 300 cm<sup>-1</sup>.....</i>	<b>S9</b>
<i>Figure S2: Comparison between the cross-sections (<math>\Delta j = 2</math>) computed for C<sub>4</sub> molecule due to its collision with para and ortho H<sub>2</sub> for different transitions.....</i>	<b>S9</b>
<i>Figure S3: Cross-sections for the rotational excitation transitions (<math>\Delta j = 2</math>) of collision of C<sub>4</sub> with ortho H<sub>2</sub> till energy range of 300 cm<sup>-1</sup>.....</i>	<b>S10</b>
<i>Figure S4: Cross-sections for the rotational excitation transitions (1-N) of collision of C<sub>4</sub> with para H<sub>2</sub> till energy range of 300 cm<sup>-1</sup>.....</i>	<b>S10</b>
<i>Figure S5: PES at various angular coordinates (<math>\phi, \theta_2, \theta_1, R</math>) with respect to R.....</i>	<b>S11</b>
<i>Figure S6: Variation of R (optimised) with respect to <math>\theta_2</math> vs <math>\theta_1</math> at <math>\phi = 0^\circ</math> .....</i>	<b>S11</b>

**Table S1: Data of rate coefficients of excitation transitions for the comparison of *para* H<sub>2</sub> and *ortho* H<sub>2</sub> as a function of temperature.**

T (K)	<i>para</i> -H <sub>2</sub>			<i>ortho</i> -H <sub>2</sub>		
	1-3	1-5	1-7	1-9	1-3	1-5
1	9.31E-12	5.42E-14	4.76E-17	6.67E-21	1.03E-11	7.23E-14
2	4.15E-11	2.39E-12	5.87E-14	6.29E-16	4.34E-11	3.22E-12
3	6.57E-11	8.55E-12	6.51E-13	2.89E-14	6.93E-11	1.12E-11
4	8.07E-11	1.61E-11	2.2E-12	1.98E-13	8.67E-11	2.07E-11
5	9E-11	2.36E-11	4.58E-12	6.36E-13	9.87E-11	2.97E-11
6	9.61E-11	3.04E-11	7.5E-12	1.39E-12	1.07E-10	3.77E-11
7	1E-10	3.63E-11	1.07E-11	2.44E-12	1.13E-10	4.45E-11
8	1.03E-10	4.16E-11	1.39E-11	3.74E-12	1.17E-10	5.03E-11
9	1.05E-10	4.61E-11	1.71E-11	5.21E-12	1.21E-10	5.53E-11
10	1.06E-10	5.01E-11	2.02E-11	6.8E-12	1.23E-10	5.96E-11
11	1.07E-10	5.36E-11	2.32E-11	8.46E-12	1.25E-10	6.32E-11
12	1.07E-10	5.67E-11	2.59E-11	1.01E-11	1.26E-10	6.63E-11
13	1.07E-10	5.94E-11	2.85E-11	1.18E-11	1.27E-10	6.9E-11
14	1.07E-10	6.18E-11	3.09E-11	1.34E-11	1.27E-10	7.13E-11
15	1.07E-10	6.38E-11	3.3E-11	1.5E-11	1.27E-10	7.32E-11
16	1.07E-10	6.56E-11	3.5E-11	1.65E-11	1.28E-10	7.48E-11
17	1.07E-10	6.72E-11	3.68E-11	1.8E-11	1.27E-10	7.62E-11
18	1.06E-10	6.85E-11	3.84E-11	1.93E-11	1.27E-10	7.73E-11
19	1.06E-10	6.96E-11	3.98E-11	2.05E-11	1.26E-10	7.82E-11
20	1.05E-10	7.05E-11	4.11E-11	2.17E-11	1.26E-10	7.89E-11
21	1.04E-10	7.13E-11	4.23E-11	2.28E-11	1.25E-10	7.95E-11
22	1.04E-10	7.19E-11	4.33E-11	2.38E-11	1.24E-10	7.99E-11
23	1.03E-10	7.23E-11	4.42E-11	2.47E-11	1.23E-10	8.02E-11
24	1.02E-10	7.27E-11	4.5E-11	2.55E-11	1.22E-10	8.03E-11
25	1.01E-10	7.29E-11	4.56E-11	2.62E-11	1.21E-10	8.03E-11
26	1E-10	7.31E-11	4.62E-11	2.69E-11	1.2E-10	8.03E-11
27	9.92E-11	7.31E-11	4.67E-11	2.75E-11	1.19E-10	8.01E-11
28	9.82E-11	7.31E-11	4.71E-11	2.81E-11	1.18E-10	7.99E-11
29	9.72E-11	7.3E-11	4.74E-11	2.86E-11	1.17E-10	7.96E-11
30	9.62E-11	7.28E-11	4.77E-11	2.9E-11	1.15E-10	7.93E-11
31	9.52E-11	7.26E-11	4.79E-11	2.94E-11	1.14E-10	7.89E-11
32	9.42E-11	7.24E-11	4.8E-11	2.97E-11	1.13E-10	7.84E-11
33	9.32E-11	7.21E-11	4.81E-11	3E-11	1.12E-10	7.79E-11
34	9.22E-11	7.17E-11	4.82E-11	3.03E-11	1.1E-10	7.74E-11
35	9.11E-11	7.13E-11	4.82E-11	3.05E-11	1.09E-10	7.68E-11
36	9.01E-11	7.09E-11	4.82E-11	3.07E-11	1.08E-10	7.62E-11
37	8.91E-11	7.05E-11	4.81E-11	3.08E-11	1.07E-10	7.56E-11
38	8.81E-11	7E-11	4.8E-11	3.09E-11	1.05E-10	7.5E-11
39	8.71E-11	6.95E-11	4.79E-11	3.1E-11	1.04E-10	7.44E-11
40	8.61E-11	6.91E-11	4.78E-11	3.11E-11	1.03E-10	7.37E-11
41	8.51E-11	6.85E-11	4.76E-11	3.12E-11	1.01E-10	7.3E-11

42	8.41E-11	6.8E-11	4.74E-11	3.12E-11	1E-10	7.23E-11	5.23E-11	3.33E-11
43	8.31E-11	6.75E-11	4.72E-11	3.12E-11	9.89E-11	7.17E-11	5.2E-11	3.33E-11
44	8.22E-11	6.7E-11	4.7E-11	3.12E-11	9.77E-11	7.1E-11	5.16E-11	3.32E-11
45	8.12E-11	6.64E-11	4.68E-11	3.12E-11	9.65E-11	7.03E-11	5.13E-11	3.31E-11
46	8.03E-11	6.59E-11	4.66E-11	3.12E-11	9.53E-11	6.96E-11	5.09E-11	3.3E-11
47	7.94E-11	6.53E-11	4.63E-11	3.11E-11	9.41E-11	6.89E-11	5.06E-11	3.29E-11
48	7.85E-11	6.48E-11	4.61E-11	3.11E-11	9.29E-11	6.82E-11	5.02E-11	3.27E-11
49	7.76E-11	6.42E-11	4.58E-11	3.1E-11	9.17E-11	6.75E-11	4.98E-11	3.26E-11
50	7.67E-11	6.36E-11	4.55E-11	3.09E-11	9.06E-11	6.68E-11	4.94E-11	3.24E-11
51	7.58E-11	6.31E-11	4.52E-11	3.09E-11	8.95E-11	6.61E-11	4.9E-11	3.23E-11
52	7.5E-11	6.25E-11	4.49E-11	3.08E-11	8.83E-11	6.54E-11	4.86E-11	3.21E-11
53	7.41E-11	6.2E-11	4.47E-11	3.07E-11	8.73E-11	6.47E-11	4.82E-11	3.19E-11
54	7.33E-11	6.14E-11	4.44E-11	3.06E-11	8.62E-11	6.4E-11	4.78E-11	3.17E-11
55	7.25E-11	6.09E-11	4.41E-11	3.04E-11	8.51E-11	6.34E-11	4.74E-11	3.15E-11
56	7.17E-11	6.03E-11	4.38E-11	3.03E-11	8.41E-11	6.27E-11	4.7E-11	3.13E-11
57	7.09E-11	5.98E-11	4.35E-11	3.02E-11	8.3E-11	6.2E-11	4.66E-11	3.11E-11
58	7.01E-11	5.93E-11	4.32E-11	3.01E-11	8.2E-11	6.14E-11	4.61E-11	3.09E-11
59	6.93E-11	5.87E-11	4.29E-11	2.99E-11	8.1E-11	6.07E-11	4.57E-11	3.07E-11
60	6.86E-11	5.82E-11	4.26E-11	2.98E-11	8E-11	6.01E-11	4.53E-11	3.05E-11
61	6.78E-11	5.77E-11	4.23E-11	2.97E-11	7.91E-11	5.94E-11	4.49E-11	3.03E-11
62	6.71E-11	5.72E-11	4.2E-11	2.95E-11	7.81E-11	5.88E-11	4.45E-11	3.01E-11
63	6.64E-11	5.67E-11	4.16E-11	2.94E-11	7.72E-11	5.82E-11	4.41E-11	2.98E-11
64	6.57E-11	5.62E-11	4.13E-11	2.92E-11	7.63E-11	5.76E-11	4.37E-11	2.96E-11
65	6.5E-11	5.57E-11	4.1E-11	2.91E-11	7.54E-11	5.69E-11	4.33E-11	2.94E-11
66	6.43E-11	5.52E-11	4.07E-11	2.9E-11	7.45E-11	5.63E-11	4.29E-11	2.92E-11
67	6.36E-11	5.47E-11	4.04E-11	2.88E-11	7.36E-11	5.57E-11	4.25E-11	2.9E-11
68	6.3E-11	5.42E-11	4.01E-11	2.87E-11	7.28E-11	5.52E-11	4.21E-11	2.87E-11
69	6.23E-11	5.37E-11	3.99E-11	2.85E-11	7.19E-11	5.46E-11	4.17E-11	2.85E-11
70	6.17E-11	5.32E-11	3.96E-11	2.84E-11	7.11E-11	5.4E-11	4.13E-11	2.83E-11
71	6.11E-11	5.28E-11	3.93E-11	2.82E-11	7.03E-11	5.34E-11	4.09E-11	2.81E-11
72	6.04E-11	5.23E-11	3.9E-11	2.81E-11	6.95E-11	5.29E-11	4.05E-11	2.78E-11
73	5.98E-11	5.19E-11	3.87E-11	2.79E-11	6.87E-11	5.23E-11	4.02E-11	2.76E-11
74	5.92E-11	5.14E-11	3.84E-11	2.77E-11	6.79E-11	5.18E-11	3.98E-11	2.74E-11
75	5.87E-11	5.1E-11	3.81E-11	2.76E-11	6.71E-11	5.13E-11	3.94E-11	2.72E-11
76	5.81E-11	5.05E-11	3.78E-11	2.74E-11	6.64E-11	5.07E-11	3.9E-11	2.7E-11
77	5.75E-11	5.01E-11	3.76E-11	2.73E-11	6.57E-11	5.02E-11	3.87E-11	2.67E-11
78	5.7E-11	4.97E-11	3.73E-11	2.71E-11	6.49E-11	4.97E-11	3.83E-11	2.65E-11
79	5.64E-11	4.93E-11	3.7E-11	2.7E-11	6.42E-11	4.92E-11	3.8E-11	2.63E-11
80	5.59E-11	4.88E-11	3.67E-11	2.68E-11	6.35E-11	4.87E-11	3.76E-11	2.61E-11
81	5.53E-11	4.84E-11	3.65E-11	2.67E-11	6.28E-11	4.82E-11	3.73E-11	2.59E-11
82	5.48E-11	4.8E-11	3.62E-11	2.65E-11	6.22E-11	4.77E-11	3.69E-11	2.57E-11
83	5.43E-11	4.76E-11	3.59E-11	2.64E-11	6.15E-11	4.73E-11	3.66E-11	2.55E-11
84	5.38E-11	4.72E-11	3.57E-11	2.62E-11	6.08E-11	4.68E-11	3.63E-11	2.53E-11
85	5.33E-11	4.68E-11	3.54E-11	2.61E-11	6.02E-11	4.63E-11	3.59E-11	2.51E-11
86	5.28E-11	4.65E-11	3.52E-11	2.59E-11	5.96E-11	4.59E-11	3.56E-11	2.49E-11
87	5.23E-11	4.61E-11	3.49E-11	2.58E-11	5.89E-11	4.54E-11	3.53E-11	2.47E-11
88	5.19E-11	4.57E-11	3.47E-11	2.56E-11	5.83E-11	4.5E-11	3.5E-11	2.45E-11

89	5.14E-11	4.53E-11	3.44E-11	2.55E-11	5.77E-11	4.46E-11	3.46E-11	2.43E-11
90	5.09E-11	4.5E-11	3.42E-11	2.53E-11	5.71E-11	4.41E-11	3.43E-11	2.41E-11
91	5.05E-11	4.46E-11	3.39E-11	2.52E-11	5.65E-11	4.37E-11	3.4E-11	2.39E-11
92	5E-11	4.43E-11	3.37E-11	2.51E-11	5.6E-11	4.33E-11	3.37E-11	2.37E-11
93	4.96E-11	4.39E-11	3.35E-11	2.49E-11	5.54E-11	4.29E-11	3.34E-11	2.35E-11
94	4.92E-11	4.36E-11	3.32E-11	2.48E-11	5.48E-11	4.25E-11	3.31E-11	2.33E-11
95	4.87E-11	4.32E-11	3.3E-11	2.46E-11	5.43E-11	4.21E-11	3.28E-11	2.31E-11
96	4.83E-11	4.29E-11	3.28E-11	2.45E-11	5.37E-11	4.17E-11	3.25E-11	2.29E-11
97	4.79E-11	4.26E-11	3.25E-11	2.43E-11	5.32E-11	4.13E-11	3.23E-11	2.27E-11
98	4.75E-11	4.22E-11	3.23E-11	2.42E-11	5.27E-11	4.09E-11	3.2E-11	2.26E-11
99	4.71E-11	4.19E-11	3.21E-11	2.41E-11	5.22E-11	4.05E-11	3.17E-11	2.24E-11
100	4.67E-11	4.16E-11	3.19E-11	2.39E-11	5.17E-11	4.02E-11	3.14E-11	2.22E-11

**Table S2: Data of rate coefficients of de-excitation transitions for the comparison of *para* H<sub>2</sub> and He as a function of temperature.**

T (K)	<i>para</i> -H <sub>2</sub>			He				
	3-1	5-1	7-1	9-1	3-1	5-1	7-1	9-1
5	9.58E-11	2.24E-11	4.37E-12	6.43E-13	2.30E-11	1.08E-11	5.63E-12	2.88E-12
6	9.23E-11	2.55E-11	6.27E-12	1.23E-12	2.30E-11	1.09E-11	5.73E-12	2.93E-12
7	8.88E-11	2.77E-11	8.01E-12	1.93E-12	2.30E-11	1.09E-11	5.79E-12	2.98E-12
8	8.54E-11	2.93E-11	9.56E-12	2.68E-12	2.28E-11	1.09E-11	5.84E-12	3.02E-12
9	8.24E-11	3.04E-11	1.09E-11	3.45E-12	2.26E-11	1.08E-11	5.86E-12	3.06E-12
10	7.97E-11	3.12E-11	1.21E-11	4.19E-12	2.25E-11	1.07E-11	5.88E-12	3.09E-12
11	7.73E-11	3.17E-11	1.30E-11	4.89E-12	2.23E-11	1.06E-11	5.88E-12	3.13E-12
12	7.51E-11	3.21E-11	1.39E-11	5.55E-12	2.21E-11	1.05E-11	5.88E-12	3.16E-12
13	7.31E-11	3.24E-11	1.46E-11	6.15E-12	2.19E-11	1.04E-11	5.88E-12	3.19E-12
14	7.12E-11	3.25E-11	1.52E-11	6.70E-12	2.17E-11	1.03E-11	5.87E-12	3.22E-12
15	6.95E-11	3.26E-11	1.57E-11	7.19E-12	2.15E-11	1.02E-11	5.85E-12	3.25E-12
16	6.80E-11	3.26E-11	1.61E-11	7.64E-12	2.14E-11	1.01E-11	5.84E-12	3.28E-12
17	6.65E-11	3.26E-11	1.65E-11	8.03E-12	2.12E-11	9.96E-12	5.82E-12	3.30E-12
18	6.51E-11	3.25E-11	1.67E-11	8.38E-12	2.11E-11	9.86E-12	5.81E-12	3.32E-12
19	6.38E-11	3.23E-11	1.70E-11	8.68E-12	2.09E-11	9.77E-12	5.79E-12	3.34E-12
20	6.25E-11	3.22E-11	1.71E-11	8.95E-12	2.08E-11	9.68E-12	5.77E-12	3.36E-12
21	6.13E-11	3.20E-11	1.72E-11	9.18E-12	2.06E-11	9.60E-12	5.75E-12	3.38E-12
22	6.02E-11	3.17E-11	1.73E-11	9.38E-12	2.05E-11	9.51E-12	5.73E-12	3.40E-12
23	5.91E-11	3.15E-11	1.74E-11	9.54E-12	2.04E-11	9.44E-12	5.71E-12	3.41E-12
24	5.80E-11	3.12E-11	1.74E-11	9.68E-12	2.03E-11	9.36E-12	5.69E-12	3.43E-12
25	5.70E-11	3.09E-11	1.74E-11	9.80E-12	2.02E-11	9.29E-12	5.67E-12	3.44E-12
26	5.60E-11	3.06E-11	1.74E-11	9.89E-12	2.01E-11	9.22E-12	5.66E-12	3.45E-12
27	5.50E-11	3.03E-11	1.73E-11	9.96E-12	2.00E-11	9.15E-12	5.64E-12	3.46E-12
28	5.40E-11	3.00E-11	1.73E-11	1.00E-11	1.99E-11	9.09E-12	5.62E-12	3.47E-12
29	5.31E-11	2.97E-11	1.72E-11	1.01E-11	1.98E-11	9.03E-12	5.60E-12	3.48E-12
30	5.22E-11	2.94E-11	1.71E-11	1.01E-11	1.97E-11	8.97E-12	5.58E-12	3.49E-12
31	5.13E-11	2.90E-11	1.70E-11	1.01E-11	1.96E-11	8.92E-12	5.56E-12	3.50E-12
32	5.04E-11	2.87E-11	1.69E-11	1.01E-11	1.95E-11	8.86E-12	5.55E-12	3.51E-12

33	4.96E-11	2.83E-11	1.68E-11	1.01E-11	1.95E-11	8.81E-12	5.53E-12	3.51E-12
34	4.88E-11	2.80E-11	1.66E-11	1.01E-11	1.94E-11	8.76E-12	5.51E-12	3.52E-12
35	4.80E-11	2.76E-11	1.65E-11	1.00E-11	1.93E-11	8.71E-12	5.50E-12	3.53E-12
36	4.72E-11	2.73E-11	1.63E-11	9.98E-12	1.92E-11	8.67E-12	5.48E-12	3.53E-12
37	4.64E-11	2.70E-11	1.62E-11	9.94E-12	1.92E-11	8.62E-12	5.46E-12	3.54E-12
38	4.57E-11	2.66E-11	1.60E-11	9.89E-12	1.91E-11	8.58E-12	5.45E-12	3.54E-12
39	4.49E-11	2.63E-11	1.59E-11	9.83E-12	1.90E-11	8.54E-12	5.43E-12	3.54E-12
40	4.42E-11	2.59E-11	1.57E-11	9.78E-12	1.90E-11	8.50E-12	5.42E-12	3.55E-12
41	4.35E-11	2.56E-11	1.56E-11	9.71E-12	1.89E-11	8.46E-12	5.40E-12	3.55E-12
42	4.28E-11	2.53E-11	1.54E-11	9.65E-12	1.89E-11	8.42E-12	5.39E-12	3.55E-12
43	4.22E-11	2.50E-11	1.52E-11	9.58E-12	1.88E-11	8.38E-12	5.38E-12	3.56E-12
44	4.15E-11	2.46E-11	1.51E-11	9.50E-12	1.88E-11	8.35E-12	5.36E-12	3.56E-12
45	4.09E-11	2.43E-11	1.49E-11	9.43E-12	1.87E-11	8.32E-12	5.35E-12	3.56E-12
46	4.03E-11	2.40E-11	1.47E-11	9.35E-12	1.87E-11	8.28E-12	5.33E-12	3.56E-12
47	3.97E-11	2.37E-11	1.46E-11	9.27E-12	1.86E-11	8.25E-12	5.32E-12	3.56E-12
48	3.91E-11	2.34E-11	1.44E-11	9.20E-12	1.86E-11	8.22E-12	5.31E-12	3.56E-12
49	3.85E-11	2.31E-11	1.43E-11	9.11E-12	1.85E-11	8.19E-12	5.30E-12	3.56E-12
50	3.79E-11	2.28E-11	1.41E-11	9.03E-12	1.85E-11	8.16E-12	5.28E-12	3.56E-12
51	3.74E-11	2.25E-11	1.39E-11	8.95E-12				
52	3.68E-11	2.22E-11	1.38E-11	8.87E-12				
53	3.63E-11	2.19E-11	1.36E-11	8.79E-12				
54	3.58E-11	2.16E-11	1.35E-11	8.70E-12				
55	3.52E-11	2.13E-11	1.33E-11	8.62E-12				
56	3.47E-11	2.11E-11	1.32E-11	8.54E-12				
57	3.43E-11	2.08E-11	1.30E-11	8.46E-12				
58	3.38E-11	2.05E-11	1.29E-11	8.37E-12				
59	3.33E-11	2.03E-11	1.27E-11	8.29E-12				
60	3.29E-11	2.00E-11	1.26E-11	8.21E-12				
61	3.24E-11	1.98E-11	1.24E-11	8.13E-12				
62	3.20E-11	1.95E-11	1.23E-11	8.05E-12				
63	3.15E-11	1.93E-11	1.21E-11	7.97E-12				
64	3.11E-11	1.91E-11	1.20E-11	7.89E-12				
65	3.07E-11	1.88E-11	1.19E-11	7.81E-12				
66	3.03E-11	1.86E-11	1.17E-11	7.73E-12				
67	2.99E-11	1.84E-11	1.16E-11	7.66E-12				
68	2.95E-11	1.82E-11	1.15E-11	7.58E-12				
69	2.91E-11	1.79E-11	1.14E-11	7.50E-12				
70	2.88E-11	1.77E-11	1.12E-11	7.43E-12				
71	2.84E-11	1.75E-11	1.11E-11	7.36E-12				
72	2.80E-11	1.73E-11	1.10E-11	7.28E-12				
73	2.77E-11	1.71E-11	1.09E-11	7.21E-12				
74	2.74E-11	1.69E-11	1.07E-11	7.14E-12				
75	2.70E-11	1.67E-11	1.06E-11	7.07E-12				
76	2.67E-11	1.65E-11	1.05E-11	7.00E-12				
77	2.64E-11	1.63E-11	1.04E-11	6.93E-12				
78	2.60E-11	1.62E-11	1.03E-11	6.86E-12				
79	2.57E-11	1.60E-11	1.02E-11	6.79E-12				

80	2.54E-11	1.58E-11	1.01E-11	6.73E-12
81	2.51E-11	1.56E-11	9.96E-12	6.66E-12
82	2.48E-11	1.54E-11	9.86E-12	6.60E-12
83	2.45E-11	1.53E-11	9.75E-12	6.53E-12
84	2.43E-11	1.51E-11	9.65E-12	6.47E-12
85	2.40E-11	1.49E-11	9.55E-12	6.41E-12
86	2.37E-11	1.48E-11	9.45E-12	6.35E-12
87	2.34E-11	1.46E-11	9.36E-12	6.29E-12
88	2.32E-11	1.45E-11	9.26E-12	6.23E-12
89	2.29E-11	1.43E-11	9.17E-12	6.17E-12
90	2.27E-11	1.42E-11	9.08E-12	6.11E-12
91	2.24E-11	1.40E-11	8.99E-12	6.05E-12
92	2.22E-11	1.39E-11	8.90E-12	6.00E-12
93	2.19E-11	1.37E-11	8.81E-12	5.94E-12
94	2.17E-11	1.36E-11	8.72E-12	5.89E-12
95	2.15E-11	1.34E-11	8.64E-12	5.83E-12
96	2.12E-11	1.33E-11	8.55E-12	5.78E-12
97	2.10E-11	1.32E-11	8.47E-12	5.72E-12
98	2.08E-11	1.30E-11	8.39E-12	5.67E-12
99	2.06E-11	1.29E-11	8.31E-12	5.62E-12
100	2.04E-11	1.28E-11	8.23E-12	5.57E-12

**Table S3:** Python program for generating PES.

Program for generating PES	Analytical expression
<pre> # Import math Library import math; import os; path = os.getcwd() print(path) for l in range (0,1,30):     phi = int(l)     directory2 = path+ "/" + "%s"%(str(l))     if not os.path.exists(directory2):         os.makedirs(directory2)     os.chdir(directory2) for k in range (0,1,30):     theta2 = int(k)     directory1 = directory2+ "/" + "%s"%(str(k))     if not os.path.exists(directory1):         os.makedirs(directory1)     os.chdir(directory1) for i in range (0,1,15):     theta1 = int(i)     directory = path+ "/" + "%s"%(str(i))     if not os.path.exists(directory):         os.makedirs(directory)     os.chdir(directory) for i in range (76):     R=1/10.0+2.5     r1 = 1.9534     r2 = 0.6445     rh = 0.3714     a1 = math.sin(math.radians(theta1))*math.sin(math.radians(phi))     a2 = math.sin(math.radians(theta1))*math.cos(math.radians(phi))     a3 = math.cos(math.radians(theta1))     b1 = math.sin(math.radians(theta2))     b2 = math.cos(math.radians(theta2))     b11=R-rh*b2     r21=R+rh*b2     f= open("%d.gif" % (i), "w+")     f.write("%%%\nprocshared=4     %%mem=10GB     %%ckh=%d_%d_%d.chk     # CCSD=(T,SaveAmplitudes,ReadAmplitudes)/aug-cc-pVTZ     R = %d, phi=%d, theta2=%d, theta1=%d,     0 3     C      %.4f    %.4f    %.4f     C      %.4f    %.4f    %.4f     C      %.4f    %.4f    %.4f     C      %.4f    %.4f    %.4f     H      0.0000   %.4f    %.4f     H      0.0000   %.4f    %.4f     </pre>	<p><i>General Expression:</i></p> $  \begin{aligned}  & C \quad r1 * \sin(\theta_1) * \sin(\phi) \quad r1 * \sin(\theta_1) * \cos(\phi) \quad r1 * \cos(\theta_1) \\  & C \quad r2 * \sin(\theta_1) * \sin(\phi) \quad r2 * \sin(\theta_1) * \cos(\phi) \quad r2 * \cos(\theta_1) \\  & C \quad -r2 * \sin(\theta_1) * \sin(\phi) \quad -r2 * \sin(\theta_1) * \cos(\phi) \quad -r2 * \cos(\theta_1) \\  & C \quad -r1 * \sin(\theta_1) * \sin(\phi) \quad -r1 * \sin(\theta_1) * \cos(\phi) \quad -r1 * \cos(\theta_1) \\  & H \quad 0.0000 \quad rh * \sin(\theta_2) \quad R + rh * \cos(\theta_2) \\  & H \quad 0.0000 \quad rh * \sin(\theta_2) \quad R - rh * \cos(\theta_2)  \end{aligned}  $ <p><i>Stationary point (Global Minimum)</i>  <math>\phi, \theta_2, \theta_1 = 0^\circ, 90^\circ, 90^\circ</math> and <math>R = 3.4 \text{ \AA}</math></p>

```

"""%(phi,theta2,theta1,R,phi,theta2,theta1,
r1*a1,r1*a2,r1*a3, r2*a1,r2*a2,r2*a3, -r2*a1,-r2*a2,-r2*a3, -r1*a1,-r1*a2,-r1*a3,rh*b1,r1l,-
rh*b1,r2l)

f.close()
os.chdir(directory)
os.chdir(directory1)
os.chdir(directory2)

```

**Table S4:** *Ab initio* energies ( $\text{C}_4\text{-H}_2$ ) at various geometries compared to recreated PES (from radial terms).

Geometry ( $\phi, \theta_2, \theta_1, R$ )	Ab initio energy	Recreated PES (from radial terms)
$0^\circ, 90^\circ, 90^\circ, 3.4 \text{ \AA}$	-147.79	-147.47
$0^\circ, 0^\circ, 0^\circ, 5.4 \text{ \AA}$	-144.83	-144.49
$0^\circ, 90^\circ, 0^\circ, 5.9 \text{ \AA}$	-18.78	-17.89

**Table S5:** Computed properties of  $\text{C}_4$  compared to previous literature.

Properties ( $\text{C}_4$ )	Current work	Previous Literature
Vibrational Frequencies ( $\text{cm}^{-1}$ )	CCSD(T)/aug-cc-pVQZ (Harmonic) No. Freq in $\text{cm}^{-1}$ [D] (mode) 1. 2107 [1] (stretching $\Sigma_g$ ) 2. 1596 [1] (stretching $\Sigma_u$ ) 3. 942 [1] (stretching $\Sigma_g$ ) 4. 369 [2] (bending $\Pi_g$ ) 5. 168 [2] (bending $\Pi_u$ )	Experimental <sup>1</sup> : No. Freq in $\text{cm}^{-1}$ 1. 2057 2. 1549 3. N.A. 4. 323 5. 160
Bond lengths ( $\text{\AA}$ )	1.2890 (inner) 1.3089 (outer) (CCSD(T)/CBS(DTQ))	Experimental: 1.304 (all same) <sup>1</sup> 1.3167 (inner) 1.2960 (outer) <sup>2</sup> 1.2840 (inner) 1.3060 (outer) <sup>3</sup>

1. "National Institute of Standards and Technology | NIST." NIST, 22 Dec. 2023, [www.nist.gov](http://www.nist.gov).
2. Lique, François, et al., *Phys. Chem. Chem. Phys.*, 12, 15672-15680 (2010).
3. Van Orden, Alan, et al., *Chem. Rev.*, 98, 2313-2358 (1998).

**Figure S1:** Cross-sections for the rotational excitation ( $1-N$ ) transitions of collision of  $\text{C}_4$  with *ortho* –  $\text{H}_2$  till energy range of  $300 \text{ cm}^{-1}$ .

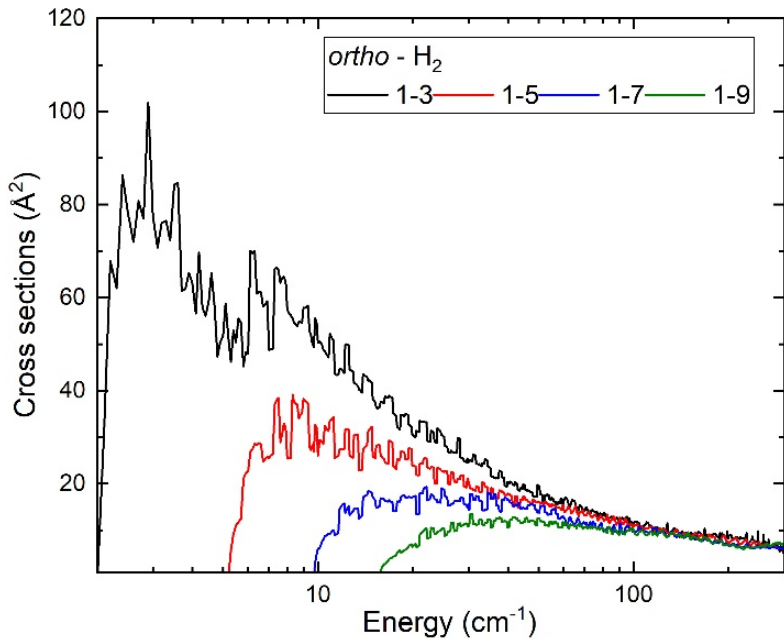


**Figure S2:** Comparison between the cross-sections ( $\Delta j = 2$ ) computed for  $\text{C}_4$  molecule due to its collision with *para* and *ortho* –  $\text{H}_2$  for different transitions as shown: Solid corresponds to *ortho* –  $\text{H}_2$  while dotted corresponds to *para* –  $\text{H}_2$ .

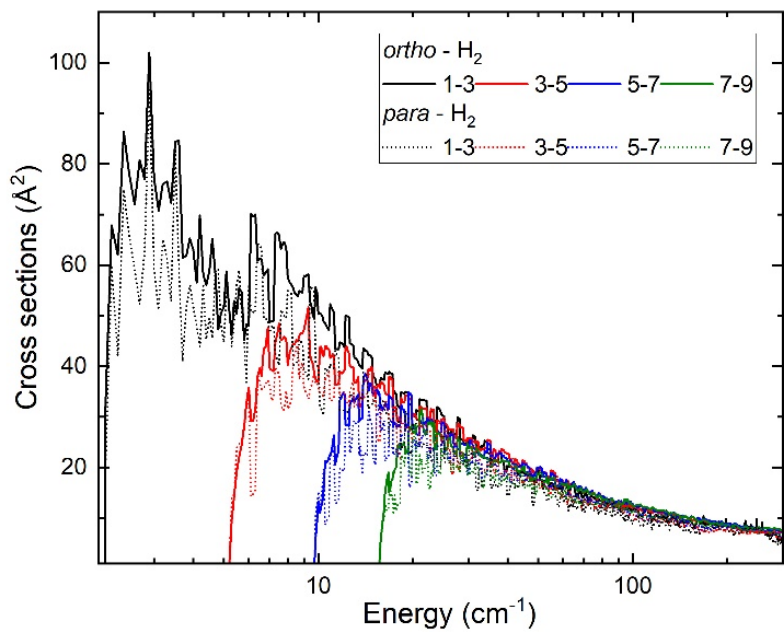


Figure S3: Cross-sections for the rotational excitation transitions ( $\Delta j = 2$ ) of collision of C<sub>4</sub> with *ortho* – H<sub>2</sub> till energy range of 300 cm<sup>-1</sup>.

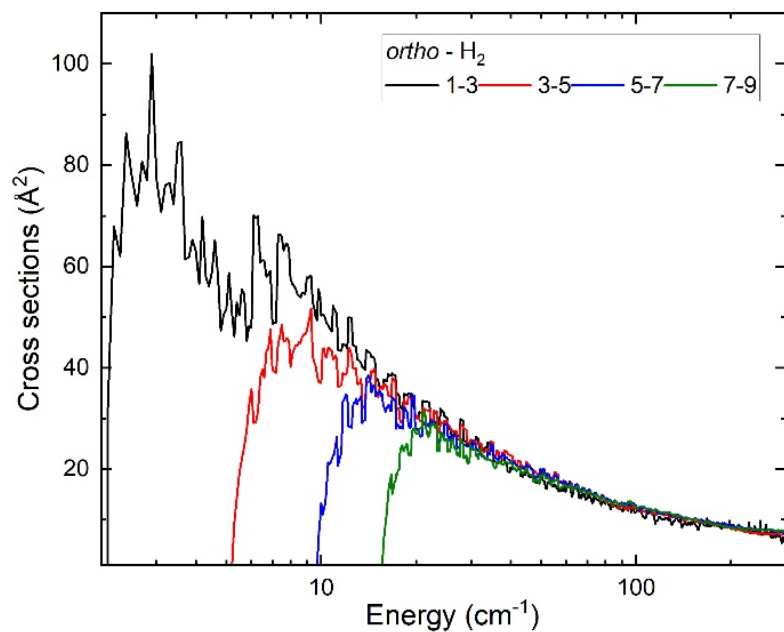


Figure S4: Cross-sections for the rotational excitation transitions (1-N) of collision of C<sub>4</sub> with *para* – H<sub>2</sub> till energy range of 300 cm<sup>-1</sup>.

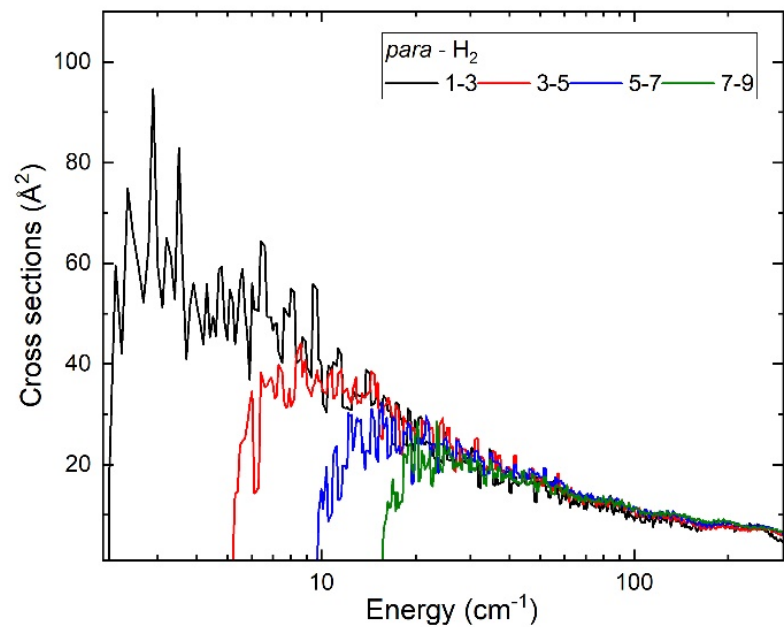


Figure S5: PES at various angular coordinates ( $\phi, \theta_2, \theta_1, R$ ) with respect to R.

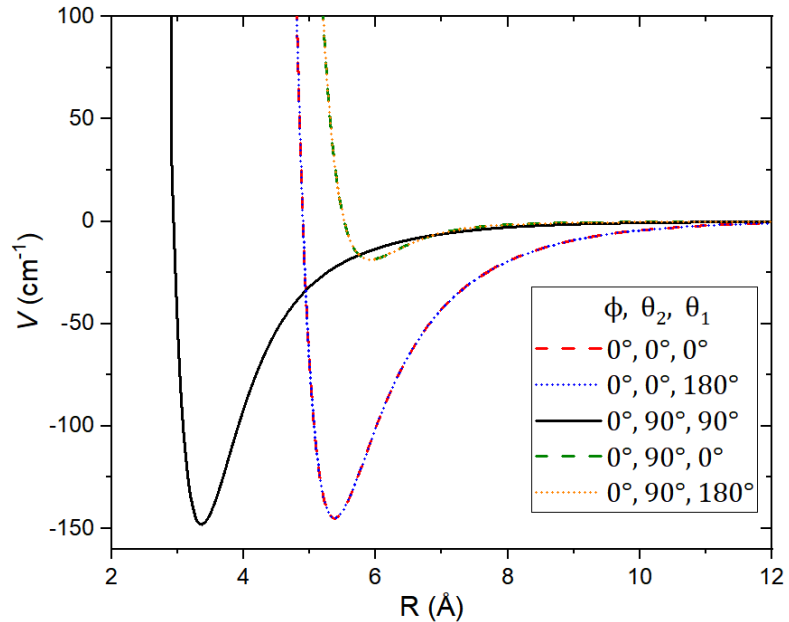


Figure S6: Variation of R (optimised) with respect to  $\theta_2$  vs  $\theta_1$  at  $\phi = 0^\circ$ .

